Review on Structure Detection and Speckle Filtering on ERS-1 Images

Yves-Louis Desnos, Valeria Matteini[1]

European Space Agency, ESTEC
P.O.Box 299 - 2200 AG Noordwijk - The Netherlands
Tel: +31-1719-84927 FAX: +31-1719-84596

ABSTRACT

A comparison between different nonlinear speckle filters for SAR images is presented in this paper. The performance's evaluation was made testing an algorithm of edge detection, based on ratio operators, applied on SAR data taken by ERS-1, the first European Remote Sensing satellite launched successfully by ESA on July 1991. The capability of structure detection, which is improved by a speckle filtering process, improves further on taking into account the multitemporal informations available from the satellite. Considering the limitations of the analyzed filters and the good results achieved using the ratio edge extractor, an adaptive speckle filter has been implemented based on both geometrical and statistical properties of the local area. The procedure uses a modified version of the generalized Lee's filter and the pixel value is replaced computing the local coefficient of variation on adaptive windows. The shape of the processing window is selected using geometrical operators that detect edges and lines in the scene. This allows to achieve a very good smoothing power in the homogeneous areas preserving, at the same time, structures and textures. In particular the filter maintains the local mean value and doesn't blur edges keeping unchanged the point target responses. Comparisons with three filters widely used in speckle smoothing are performed on ERS-1 data. The test images, collected in August-October 1991, refer to Flevoland area, a polder close to Amsterdam. The good results obtained and the evident improvements with respect to the classic algorithms are presented and discussed.

INTRODUCTION

The Synthetic Aperture Radar (SAR) is one of the most promising and helpful instruments for monitoring land features. Structures in a SAR image feed important contextual information useful to detect and to classify environmental entities such as: vegetated areas, agricultural fields, residential complexes, industrial areas. Unfortunately, because of the coherent nature of the illumination, radar images are speckled and the intrinsic field texture is often not significant or masked by noise effects. When analysing SAR data the first step is smoothing speckle while, at the same time, preserving features like edges and fine details. In literature we found a lot of filters that have the aim to reduce the speckle noise.

General filters like the median or box filters produce a very good smoothing effect but, when they are efficient in homogeneous areas, they destroy profiles and blur edges. Instead the geometric filter (T.R. Crimmins, 1985) uses a different approach in speckle noise reduction: the filter smooths speckle taking into consideration the image's morphology with an alternative sequence of dilatation and erosions.

Given the special characteristics of the radar images, these filters, based on euristic criterious, are not always suitable for speckled images. Best results are obtained considering a mathematical model for signal and noise. From the statistical properties of the speckle (J.W. Goodman, Nov. 1976) several non-linear filters have been proposed based on additive and multiplicative noise models.

The most known filters in this field such as the Frost (V.S. Frost, J.A. Stiles, K.S. Shanmugan, e J.C. Holtzman, Mar. 1982), Lee (J.S. Lee, March 1980) or Kuan (T. Kuan, A. Sawchuk, T. Strand, P. Chavel, Mar. 1985) are adaptive based on the local statistics and they reduce the speckle noise as a function of the degree of heterogeneity measured by the local coefficient of variation.

In presence of point targets and structural features likes lines or edges, if fixed windows are used, the speckle filtering is poor.

For this reason adaptive procedures have been proposed by Lee (J.S. Lee, 1983) and Nezry *et al.* (E. Nezry, A. Lopes, R.Touzi, Jun. 1991): these filters use local statistics

[1] Graduate from the University of Florence has worked as stagies at ESA/ESTEC.

but also take into account geometrical informations we can achieve applying edge operators on the image.
We have tested a modification of the procedure presented in (E. Nezry, A. Lopes, R.Touzi, Jun. 1991). The filter is "driven" from the geometrical operators, used in an interesting edge detector proposed by Touzi *et al.* (R. Touzi, A. Lopes, P. Bousquet, Nov. 1988) and based on the ratio pixel values, that allow us to choose the best neighbourhood where to compute the coefficient of variation and apply an "enhanced" generalized Lee filter version. In this way it is possible to obtain a very high speckle reduction and a good texture preservation.
The filter has been compared with three filters following different approaches in speckle reduction techniques and in particular the median filter, the geometric filter and the Lee filter.
In the first part of the work these algorithms have been applied on the images and then the ratio edge detector has been used. The application of the edge extractor allowed us to point out characteristics and differences between the filters.
In Section I is presented the ratio edge detector we have used to evaluate the performance of the three filters. This algorithm is suitable for images corrupted by multiplicative noise (like is this case) and allows to select automatically the decision thresholds. In Section II the results of these applications on ERS-1 images are explained. Also the results of the edge detection using multitemporal data are shown. In Section III the statistical and geometrical filter is described in details. In particular, the local coefficient of variation is defined and the "Enhanced Lee Filter" and the geometrical operators are presented. In Section IV a comparison between the filters was made considering some criteria of interest like the mean tonal preservation, the noise reduction power and the point target responce maintenance.

1. THE RATIO EDGE DETECTOR

Speckle has its origin in the interference of dephased but coherent wavelets, backscattered from a rough surface on the scale of the wavelength. Since speckle is modelled as multiplicative, an approximation to the gradient (usually in the form of differenced neighbourhood averages or weighted averages or, like in Robert's and Sobel's operators, using convolution masks) gives often unsatisfactory results if applied to SAR images. In fact the gradient distribution is larger if the mean power, computed in a homogeneous area, is larger. Also this kind of operators detects more false alarms within brighter homogeneous area (R. Touzi, A. Lopes, P. Bousquet, Nov. 1988). Bovik [1] and Touzi (R. Touzi, A. Lopes, P. Bousquet, Nov. 1988) consider it more useful to face the edge detection as an estimation/thresholding problem.

The edge detector proposed by Touzi *et al.* is based on the ratio between pixel values so that the alarm rate is constant. Moreover it is possible to derive the probability distribution of the image obtained applying the edge detector.
Given a L-look power SAR image, the probability density function (pdf) of the power received from an homogeneous area is given by (cf.(R. Touzi, A. Lopes, P. Bousquet, Nov. 1988)):

$$p\,(x/P_0) = \frac{1}{\Gamma\,(L)}\left(\frac{P_0}{L}\right)^{-L} x^{L-1}\exp\left(-\frac{xL}{P_0}\right) \qquad (1)$$

where x is the random pixel value, $E(x) = P_0$ and P_0 is the mean power of the distributed target proportional to the backscattering coefficient σ^0.
The ratio edge detector is defined as the ratio of the average (arithmetic for a power image, quadratic for an amplitude image) of pixel values of two non-overlapping neighbourhood s on opposite sides of the point.
Because ERS-1 images are defined in amplitude the average X of N independent pixels is:

$$X = \sqrt{\frac{1}{N}\sum_{i=1}^{N} X_i^2}$$

where X_i is the amplitude value of the i-th pixel.
The ratio value for a pixel is defined as $R = X_1/X_2$ where X_1 and X_2 are the average values computed over the two neighbourhood s on the opposite side of the point.
Fixed two decision thresholds T_1 and T_2 the considered point is assigned to:
- the edges if $R < T_1$ or $R > T_2$;
- the homogeneous area in the other case.

Clearly, the performance of the ratio edge detector depends on the choice of the two decision thresholds T_1, T_2 ($T_1 \leq 1$, $T_2 \geq 1$). In order to have a symmetrical operator T_2 is taken equal to $1/T_1$.
Practically in the algorithm we calculate the ratio value and then we choose for processing the ratio detector r ($0 \leq r \leq 1$) with:

$r = R$ if $R \leq 1$
$r = 1/R$ if $R > 1$

The conditional pdf of the bounded ratio detector r is given by:

$$p(r/P) = \frac{2\,\Gamma(2NL)}{\Gamma(NL)^2}\cdot\left[\frac{P^{NL}}{(r^n+P)^{2NL}} + \frac{(1/P)^{NL}}{(r^n+1/P)^{2NL}}\right]\cdot r^{2NL-1} \qquad (2)$$

where $P = P_1/P_2$ is the ratio between the mean powers P_1 and P_2.
If we define $C = \min[P, 1/P]$ the pdf is a function of C, the

contrast ratio of the homogeneous areas, of the number of pixels N in each homogeneous area and of the number of looks L.
So, given a decision threshold T, the conditional probability of detection Pd with a boundary between two homogeneous regions of a contrast ratio $C = P_1/P_2$ is:

$$Pd\,(T,C) = Prob\,(r < T/C) = \int_0^T p\,(r/C)\,dr \qquad (3)$$

The probability of false alarm Pfa is defined:

$$Pfa\,(T) = Pd\,(T,1) \qquad (4)$$

From the (4) follows that the threshold value can be chosen, by selecting a (low) Pfa for a contrast C=1. On the other hand this allows to detect boundaries between two homogeneous areas with contrast ratio C_1, with a probability given by the (3) for the threshold T and $C = C_1$. So one can fix T given a Pfa (4) or a Pd and C value (3).
Given a Pfa (as 0.01), we can notice that, the larger the neighbourhood , the higher the threshold T.

1.1 The algorithm

1) Edge orientation

We can see that performance of the edge detector improves by considering larger local neighbourhood s or processing windows. However, larger local processing windows imply a larger number of possible edge orientations. To detect most of the edges, the operator must be applied in all the possible directions. In practice, we split the window centred at a point into two contiguous regions. The split corresponds to the usual four directions. We compute the ratio value in each direction and the minimum ratio, corresponding to the most probable edge direction, is assigned to the considered point in the ratio image.
Considering the four directions an experimental relation has been established and tested in the image (R. Touzi, A. Lopes, P. Bousquet, Nov. 1988). Then the four-direction Pfa is given by:

$$Pfa_4 \cong 1 - (1 - Pfa_1)^3$$

where Pfa_1 is calculated by the (4).

2) Variable neighbourhood size

The ratio operator is less sensitive to the speckle noise with larger neighbourhood but the micro edges, detectable with small windows, may be missed. In order to select also the small edges, neighbourhood of increasing size are used.
The program processes the image with 3 different increasing window sizes. First of all we choose the threshold values T_i (i = 0...3). Then the operator is computed over the smallest window (i = 1). The *r* value is kept if it lies in the interval $[T_0, T_1]$. In the other case, the operator is computed over the successive larger window (i = 2). The *r* value is also retained if it lies in the interval $[T_1,T_2]$, in the other case the successive window is considered and so on. At the end if the *r* value is not between $[T_2,T_3]$ the pixel is assigned to homogeneous area. In Fig. 1 the algorithm is synthesised. The chosen window sizes are 3x3, 5x5, 7x7.

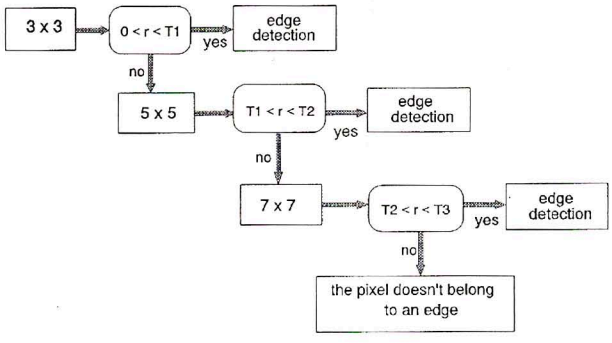

Fig. 1 - Scheme of the edge detection algorithm.

2. ALGORITHM'S APPLICATION TO ERS-1 IMAGES

Tests of the ratio detector have been performed on ERS-1 images of Flevoland fields
Data size used is 500x500 pixels for these 3 look images. Two kinds of ERS-1 products are available (N. Longon (Editor), 1991):

- VMP images: pixel spacing 12.5 meter in azimuth and ground range.
- FDP images: pixel spacing of 20 meter in ground range and 16 meter in azimuth range.

For both products the output is coded as 16 bit (integer). The edge detector has been applied to the original and filtered images. For the original image the threshold values have been taken for a Pfa = 0.01 and for $N_1L = 9$, $N_2L = 30$, $N_3L = 63$. We can notice a lot of false alarm especially detected with the smallest window on FDP images. Maybe this is due to the fact that, the real image is not indeed a 3 look image. Computing the statistical parameters in small windows the equivalent number of look found is about 2.5 - 2.7. Tests with the thresholds 0.37/0.58/0.76 computed for the new parameters values gave better results.

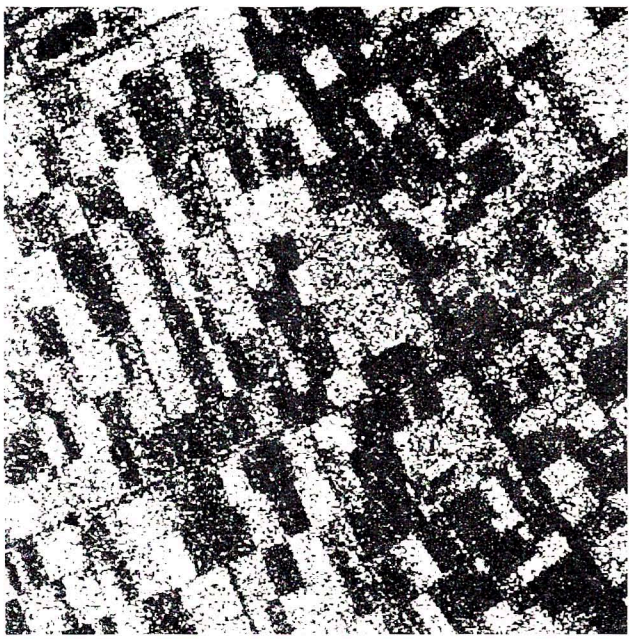

Fig. 2 - Test image in the Flevoland area.

After a speckle filtering process the distribution of the noise changes and characterizing the new distribution is very difficult especially if we use non linear filters. So in this case is not possible select automatically the thresholds. We have computed the threshold values computed using, for filtered images, the Equivalent Number of Look (ENL - defined as E(P)^2/var(P)) but the results are not good. Infact the new theoretical distribution has not been derived and the (1) is no more true. Several tests have led to the choice of a set of thresholds that allowed to obtain better results on all the filtered images. With the same thresholds values used for the original images improvements are evident and we choosed to keep fix this parameter.

In Fig. 2 is presented a test area. The results of the edge detector applied to the original and to the filtered vmp-images of a part of Flevoland are shown in Figs 3a, 3b, 3c, 3d. This permits to point out the differences between the various filtering processes.

To assess the effect of the edge detector on the images and to compare quantitatively the filters the simple figure of merit introduced by Pratt (W.K. Pratt, I.E. Abdou, May 1979) has been considered. The figure of merit utilizes a square array of pixels with a vertically oriented ramp edges in its center. It computes a mean-square distance between the ideal edge points and the real detected edges providing a penalty between smeared edges and isolated, but offset, edges. The closer to 1 is the figure of merit, the higher is the probability of good edge detection.

The test has been done using edge-maps generated on real and simulated images.

First we give a briefly description of the speckle generation techniques and then the figur of merit comparison is presented.

2.1 Speckle generation

There are different methods to simulated speckle.

Speckle generation has been done in two ways:

- straightfroward generation of a random variable in a pixel obeying the statistical properties seen in (J.W. Goodman, Nov. 1976). In this case we suppose speckle signal dependent but not correlated.
- "fully developed speckle" generation. This method takes into account the correlation between neighboring pixels (P. Dewaele, P. Wambacq, A. Ocsterlinck, Dic. 1989).

Both the methods have been implemented. We have used for the test a simulated image considering the second model, more suitable and closed to the reality than the simplified one.

According to this model the discrete complex amplitude speckle image **b**(m,n) is:

$$b\,(m,n) = \sum_i \sum_k h\,(m-i,n-k)\,E\,(i,k)\,\exp\,(j\phi\,(i,k))$$

where E(i,k) is the amplitude signal scatterer phasor for the pixel (i,k) with the phase independent and uniformly distributed, and h(m,n) is the coherent point spread function of the system defined as:

$$h\,(m,n) = sinc\left(\frac{\pi}{2}m\right)\cdot sinc\left(\frac{\pi}{2}n\right) \qquad \text{for} \quad m,n \le 2$$
$$= 0 \qquad \textit{otherwise}$$

The speckle size of the correlation region of the speckle image is approximately the size of the point spread function.

2.2 Evaluation of the results

Two images were simulated for two different edge step heights of 2.7 and 5.4 dB, typical values for contrast between fields in agricultural scenes. The figure of merit has been computed on the real and simulated boundaries and results are summarized in Table 1.

Several observations can be made looking at the table.

The *median filter* is very sensitive to the edge height, but for low contrast edges, where the signal and the noise are of the same order, the filter may erroneously replace some pixel values by wrong estimated median values. The considerable smoothing effect in the homogeneous areas re-

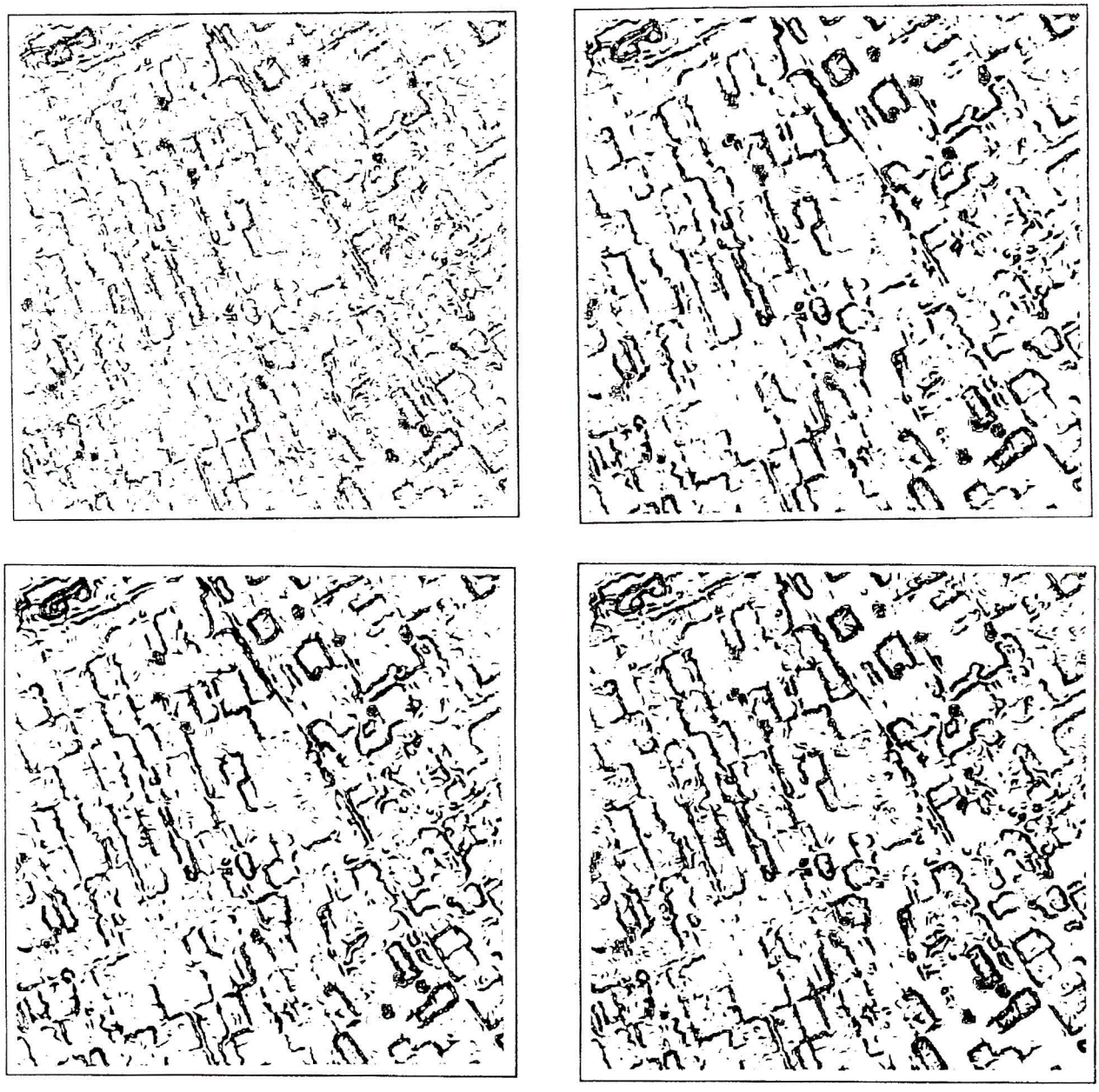

Fig. 3 - Ratio edge detection directly on the original data (a) or after a speckle filtering process: edge map of the image filtered with the Lee filter (window 7x7) (b), with the median filter (window 5x5) (c) and after 10 iterations of the geometric filter (d). In every case the threshold set used is $T_0=0, T_1=0.37, T_2=0.58, T_3=0.76$.

duces strongly the speckle but blurs weaker edges, point targets and fine details no more detectable with the edge operator. So, for big windows and low contrast the probability of good edge detection is poor.

The *Lee's filter* and the *geometric filter* gave similar results. For a contrast of about 5 dB the figure of merit is increasing with the dimension of the operator (Lee's filter) and more considerably, with the number of iterations (geometric filter).

In the case of low edge steps the effect of the thresholds is important. Considering the Lee's filter a decreasing of the f.m. can be noted changing from a 5x5 to a 7x7 processing window. Probably the better smoothing effect of larger windows in the neighbourhood of a weak edge reduces at the same time noise and contrast. This is even more evident for the geometric filter: at the 7th. iteration we obtain the highest value of the f.m. along a 2.7 dB boundary. Afterwards it decreases again. Therefore it is obvious as that the performance of the edge detector depends both on the filter and on the thresholds values. Clearly, increasing the limits rises the probability of edge detection but, at the same time, more false alarms are

Table 1: Figure of merit comparison for different filters.

	Synthetic image		Real image	
	2.7 dB	5.4 dB	2.7 dB	5.4 dB
Original	0.383577	0.743475	0.406852	0.767075
Filtered				
Lee				
3x3	0.577796	0.762510	0.574018	0.738972
5x5	0.710282	0.881982	0.655379	0.825150
7x7	0.430493	0.885691	0.456016	0.828049
9x9	0.339840	0.895237	0.355934	0.829690
Median				
3x3	0.406810	0.671085	0.403205	0.703673
5x5	0.347664	0.889284	0.364821	0.891302
7x7	0.175148	0.910936	0.154821	0.924230
Geometric				
5 iter.	0.496458	0.750804	0.509388	0.755410
6 iter.	0.537879	0.781933	0.567657	0.796199
7 iter.	0.594976	0.816700	0.608557	0.796199
8 iter.	0.536560	0.840395	0.511549	0.855757
9 iter.	0.478340	0.859713	0.458215	0.862653
10 iter.	0.393893	0.894896	0.418215	0.897525

detected. Anyway the statistical Lee's filter and the geometric filter seem to be more suitable in these cases thanks to their better adaptivity to the scene.

2.3 Multitemporal data

In the first months of its mission ERS-1 had a repeat cycle of three days. Images of the same area are available within 3 days repeat interval. This allows to investigate more deeply on the nature of lands and to gather more information about soil features changing versus time and state of the atmosphere.

Also from the edge detection point of view multitemporal data are very helpful and permit to detect more details in the scene. Therefore in order to use all the possible information available for ERS-1, the edge detector has been applied to FDP-images of the same area, but taken at different days. In Figs. 4a, 4b, 4c it is possible to see the results after applying the edge operator on data of the 20th August, 4th and 25th October. One can notice, for example, that the lake zone in the left top corner is not good recognizable in the 25th October image. Instead this is possible in the other two images. On the other hand one of the two big channels in the area is better detectable in the 25th Oct. image than in the others. The fields are better pointed out on 20th Aug., while the upper channel is good extracted on the 4th Oct.

By summing the informations of two or all the three images by simply taking the logical OR of the binary edge maps it is possible to restore almost completely the "skeleton" of the image. It's easy to verify that the detection of edges and closed contours, difficult to point out with only one image, is now feasible. The Fig. 4d indicates the final result. It's possible to notice more thicked edges in the combined image. In fact the problem of misregistration when we use the logical OR to combine the image has to be considered. We selected the area beeing carefull to take

exactly the same zone. Anyway a displacement of a pixel - due also to the various conditions of backscattering, in the different periods of the year of a reference point (however accurate it can be) - is possible.

blur edges effecting heavily the characteristic of the scene. Geometric filter preserves well edges but reduce the amplitude of points targets if they have a width comparable with the dimension of the speckle spike. For these reasons

Fig. 4 - Ratio edge detection on multitemporal data: (a) FDP_20august data, (b) FDP_4october data, (c) FDP_25october data, (d) sum of the three maps of the 4th oct., 25th oct. and 20th aug.

3. THE STATISTICAL AND GEOMETRICAL FILTER FOR ERS-1 IMAGES

3.1 Principles

It has been shown in Section II general filters like the median filter have a very good smoothing power if work in homogeneous areas, but in proximity of boundaries they adaptive filters are preferable because more suitable for preserving radiometric and textural information. The best known adaptive filters such as Lee (J.S. Lee, March 1980), Frost (V.S. Frost, J.A. Stiles, K.S. Shanmugan, e J.C. Holtzman, Mar. 1982), and Kuan (T. Kuan, A. Sawchuk, T. Strand, P. Chavel, Mar. 1985) filters are based on the local statistic of the image computed on a fixed window. The speckle is reduced as a function of the heterogeneity

measured by the coefficient of variation C_I defined as the ratio between standard deviation and mean value of an area. Near edges or in presence of point targets noise is not well reduced because the coefficient of variation can take high values when we use fixed windows. The problem of a good estimation of the local statistics around edges was partially solved by Lee (J.S. Lee, 1983) by using gradient operators. In the window, an edge is detected if one of the oriented gradient value is greater than a given threshold. The window is splitted in two parts and only the one at which the central pixel belongs is retained for local statistics computation. Considering the advantages of the ratio detector approach compared to the gradient operators (R. Touzi, A. Lopes, P. Bousquet, Nov. 1988) for SAR images, recently a different strategy has been proposed (E. Nezry, A. Lopes, R.Touzi, Jun. 1991).

In the algorithm the filtering is controlled both by the coefficient of variation and by the geometrical ratio operators extended also to the line detection case. We have implemented this algorithm applying it to an *enhanced* version of the Lee's filter (A. Lopes, R. Touzi, E. Nezry, Nov. 1990), in order to have a better assessment of the filter compared with the others previously analysed.

The scheme is based on the computation of the coefficient of variation. This parameter is a very efficient and robust index of textural informations which measures the image homogeneity. For an amplitude image, as a function of the observed coefficient of variation C_a, we can distinguish the following cases:

1) $C_a \leq C_u$: homogeneous area;
2) $C_u < C_a \leq C_{MAX}$: textured area;
3) $C_a > C_{MAX}$: presence in the area of strong scatterer or edges or linear features.

C_u usually is taken equal to the theoretical mean value C_A computed on a homogeneous area and it depends just on the number of look of the image (F.T. Ulaby, A.K. Fung, R.K. Moore). For amplitude images $C_A \approx 0.523/L$. Often we used for C_u a value slightly smaller in order not to have a strong blurring effect using the refined windows. The upper thereshold C_{MAX} has been chosen as the maximum value of the coefficient of variation computed in a homogeneous area. This allows a better texture preservation even if the user can modify this value according to the spatial resolution he wants to preserve.

In order to have a best spatial adaptivity the statistical parameter C_a is computed on variable windows determined thanks to the geometrical ratio operators we have used previously in the edge detection described in Section I.

Now the use of that operators is extended also to the case of the line detection (E. Nezry, A. Lopes, R.Touzi, Jun. 1991). As is well explaned in (A. Lopes, E. Nezry, R. Touzi, H. Laur, 1991) the new adaptive windows are selected on the base of the ratio operators that, fixed the threshold values, detect structural features. Edges between extended areas of different $\sigma^0$are modeled by 2 strips or 3 strips of mean intensities P1 and P2 with respectively N_1 and N_2 pixels. (Fig. 5).

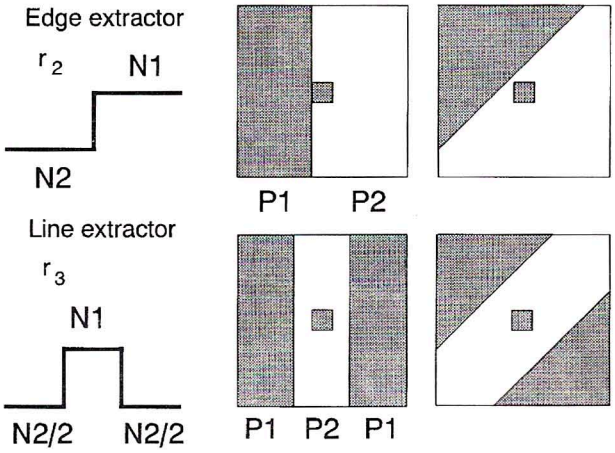

Fig. 5 - Edge and line ratio operators spatially oriented.

The corresponding detectors are:

- ratio edge $r_2 = \min(M_1/M_2, M_2/M_1)$
- ratio line $r_3 = \min(M_1'/M_2', M_2'/M_1')$

where M_1, M_2, M_1',M_2' are defined as the averaged pixel values within the subwindows of mean intensity P_1 and P_2. For an amplitude image the definition is the (1).

The most probable orientation of the feature is obtained by taking the minimum value of r_2 and r_3 computed over the usual four principal directions. An edge is detected if $r_2 < r_{2min}$ where the threshold r_{2min} is obtained from the conditional pdf (2).

Likewise the distribution probability function of $r_3 \in [0,1]$ is computed and hereafter the r_{3min} value is derived (E. Nezry, A. Lopes, R.Touzi, Jun. 1991). For an amplitude image we have:

(the equation is different because of we found some errors in (E. Nezry, A. Lopes, R.Touzi, Jun. 1991). *Besides we wrote in a different way)*

$$f(r_3) = \frac{2\Gamma(N_1L+N_2L)}{\Gamma(N_1L)\,\Gamma(N_2L)} \left[\left(\frac{P_2}{P_1}\right)^{N_1L} \left(\frac{N_2}{N_1}\right)^{N_2L} \frac{r_3^{(2N_1L-1)}}{\left(r_3^2 \cdot \frac{P_2}{P_1} + \frac{N_2}{N_1}\right)^{(N_1L+N_2L)}} + \left(\frac{P_1}{P_2}\right)^{N_1L} \left(\frac{N_1}{N_2}\right)^{N_1L} \frac{r_3^{(2N_2L-1)}}{\left(r_3^2 \cdot \frac{P_1}{P_2} + \frac{N_1}{N_2}\right)^{(N_1L+N_2L)}} \right]$$

Like for the edge detector the threshold r_{3min} is computed numerically by using the contrast ratio value $C=\min(P_1/P_2, P_2,P_1)$ and the probability of detection Pd the user wants defined as:

$$p\,(d/C) = \int_0^{r_{3min}} f\,(r_3/C)\,dr_3$$

The probability of false alarm for one direction is:

$$Pfa_1 = P\,(d/C = 1)$$

In figure 6 and 7 some cases of ratio edge and ratio line pdf for different values of N_2 and N_1 (here equal to 3) corresponding to 7x7 processing windows, are shown.
Fixed a probability of detection Pd = 95%, in Table 2 is indicated the ratio thresholds and the corresponding false alarm probabilities for some contrast values C and a 7x7 spatial operator.
The threshold values must be chosen looking both at the probability of detection Pd and at the Pfa. We can see for example that, if we choose r_{2min}=0.8, obtain at the same time a good probability of detection of boundaries with contrast ratio $C \leq 0.5$ and Pfa_4=3%.

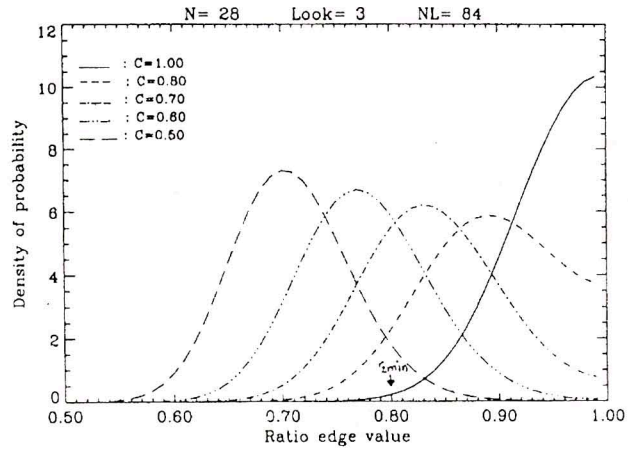

Fig. 6 - Edge probability distribution for a window 7x7.

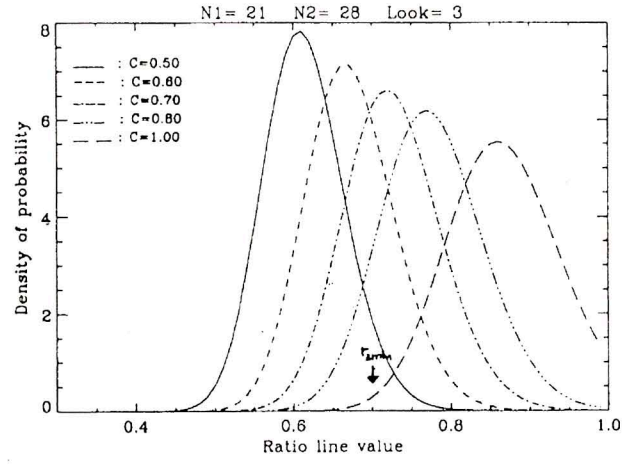

Fig. 7 - Line probability distribution for a window 7x7.

3.2 Enhancement of the Lee's filter

Given the observation z(t), the original signal x(t), the final expression of the Lee's statistical filter (J.S. Lee, May 1986) [4≤] can be written in the following form:

$$x\,(i,j) = z\,(i,j)\,w\,(i,j) + \langle z\,(i,j)\rangle \cdot (1 - w\,(i,j))$$

where $\langle z(i,j) \rangle$ is the local mean and w(i,j) is the weighting function expressed by:
with $C_I = \sigma_I/\bar{I}$ is the observed coefficient of variation. The (5) is equivalent to the Kuan filter expression (T. Kuan, A. Sawchuk, T. Strand, P. Chavel, Mar. 1985).

Table 2: Contrast ratio and threshold values for Pd = 95%. The values For C = 1 instead are given for a Pfa_1 = 1%.

	w = 7x7 N_1 = 21 N_2 = 28					
	C	**C(dB)**	**r_{2min}**	**Pfa_4**	**r_{3min}**	**Pfa_4**
Pfa = 1%	1.00	0	0.79	0.03	0.71	0.03
Pd = 95%	0.8	1.0	0.98	0.99	0.88	0.92
	0.7	1.5	0.95	0.91	0.83	0.67
	0.6	2.2	0.88	0.38	0.76	0.17
	0.5	3.0	0.80	0.03	0.70	0.02

$$w(i,j) = \left[1 - \frac{C_u^2}{C_I^2(i,j)} \right] / (1 + C_u^2) \qquad (5)$$

These filters are based on the multiplicative speckle statistic (derived beginning from a stationary mean, nonstationary variance model and additive noise (T. Kuan, A. Sawchuk, T. Strand, P. Chavel, Mar. 1987)) that assumes "fully developed" noise. This is true if a very large number of scatterers is present in a resolution cell so that it is possible to consider phase and amplitude statistically independent. In the case of built-up areas or isolated and strong point targets the filter estimate is not more valid. So a good filter should restore the mean backscatter signal in the homogeneous zones, smooth speckle without blur textural information in the heterogeneous areas, preserve point targets response when there are few and strong scatterers within a resolution cell.

According to the considerations and taking into account the remarks done in the paragraph III.1 an *enhanced* version of the filter has been proposed in (A. Lopes, R. Touzi, E. Nezry, Nov. 1990).

Computing in every processing window the local coefficient of variation C_a the amplitude pixel is estimated as:

- $x(i,j) = \overline{A}(i,j)$ if $C_a(i,j) \le C_u$
- $x(i,j) = \overline{A}(i,j)w(i,j) + z(i,j)(1-w(i,j))$ if $C_u < C_a(i,j) < C_{MAX}$
- $x(i,j) = z(i,j)$ if $C_a(i,j) \ge C_{MAX}$

where z(i,j) is the observed amplitude, $\overline{A}(i,j)$ is the mean computed on the window, w(i,j) is the weighting function defined in (5).

3.3 The algorithm (ESTEC approach)

The complete algorithm of the filter is schematized in the flow chart of Fig.8.

We have applied the *enhanced* Lee's filter, used in (A. Lopes, R. Touzi, E. Nezry, Nov. 1990) on fixed window, inside the algorithm driven by the ratio operators and coefficient of variation. The scheme is the same used in (E. Nezry, A. Lopes, R.Touzi, Jun. 1991) but here we check two times the value of C in the window, one inside the general algorithm, the other applying the *enhanced* Lee's filter in every window or subwindow selected (see Fig.9). This allows to locate more carefully the area to filter and to isolate scatterers and fine edge features.

3.3.1 Input parameters

Window size: Larger windows allow to smooth better noise and compute more precisely the coefficient of variation. It has been shown in (A. Lopes, E. Nezry, R. Touzi, H. Laur, 1991) that there is a relation between the number of incoherent samples N (and hence of the window size) and the precision of the real reflectivity value one wants to achieve. Considering the image under estimation also spatial resolution and physical dimension of the features should be taken into account. Filtering has been performed using 7x7 and 5x5 windows for VMP-images and 5x5 for FDP-images, in relationship to the different spatial resolutions of the products.

C_{MIN} and C_{MAX}: For a 3-look amplitude image an area is considered homogeneous if $C_u \le 0.294$. This is the coeffi-

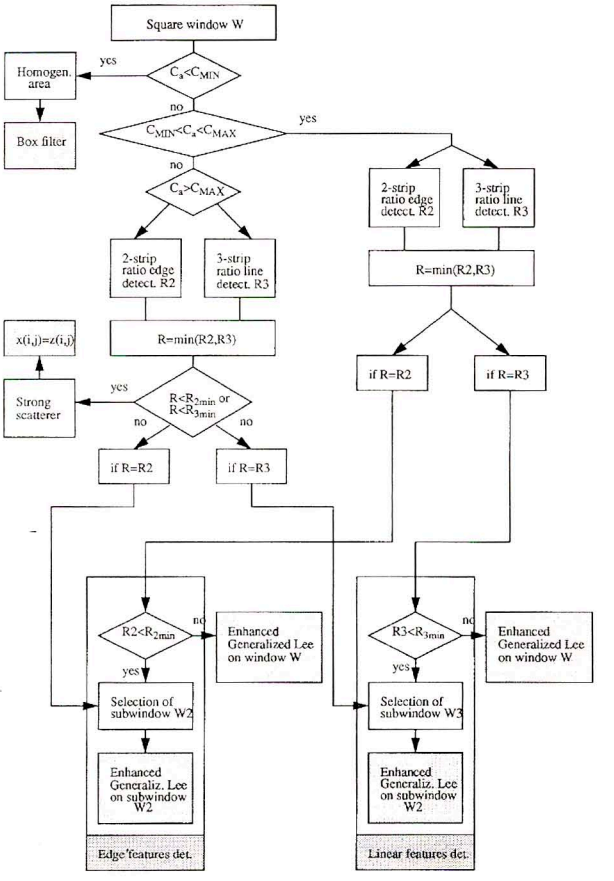

Fig. 8 - Statistical and geometrical filter's algorithm: ESTEC approach.

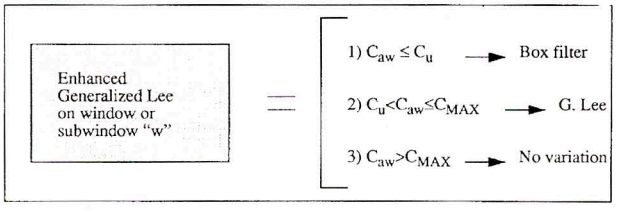

Fig 9 - Scheme of the Enhanced generalized Lee filter "box" used inside the algorithm's body.

Table 3: Mean values and ENL computed on windows 5x5 within an homogeneous area.

Image	Mean value μ	σ/μ	ENL=$((\mu/\sigma)0.523)^2$
vmp_21.dat	257.662	0.300114	3.03
Lee 5x5	257.839	0.109627	22.7
Lee 7x7	257.823	0.084972	37.9
Median 5x5	254.032	0.100730	26.9
Median 7x7	255.568	0.059472	77.3
Geometric 9 it.	260.682	0.081361	41.3
Geometric 10 it.	260.983	0.069501	56.6
ESTEC filter 7x7 C_{min}=0.29 C_{max}=0.43	257.170	0.052246	100.2
ESTEC filter 7x7 C_{min}=0.26 C_{max}=0.43	257.641	0.054085	93.5
ESTEC filter 5x5 C_{min}=0.27 C_{max}=0.5	257.543	0.083155	39.5

cient of variation called, in our case C_{MIN}. Practically, if we compute in an homogeneous area C_u using a moving window W, we found it around the mean value as a bounded gaussian function. Fig. 10a and Fig. 10b show the distribution of C_u computed on a simulated 3-look image and on a real ERS-1 zone supposed homogeneous. Because, how it's possible to notice, the results are similar, we have refered to the first one. We have selected C_{MIN} as the mean value of this distribution. The mean value is similar to the theoretical value but, when we compute the distribution of C_u on smaller window, the mean value decreases a little. So, to have good performance also using the subwindows is better take $C_{MIN} <= 0.29$. The choice of C_{MAX} is more difficult. Theoretical studies exist about this threshold in the case of intensity image (A. Lopes, E. Nezry, R. Touzi, H. Laur, 1991). In order to preserve well point targets and textural informations and given the strong smoothing effect of the filter we have selected C_{MAX} as the maximum value of the distribution of C_u compted on a simulated homogeneous area. *(Fig.10)*

4. APPLICATIONS AND RESULTS

The filter has been applied on ERS-1 images. Given a 7x7 processing window the have taken $C_{MAX} = 0.43$ and C_{MIN}= $0.29 \div 0.26$. Comparing its performance with the other filters previously analyzed we can notice considerable improvements with respect to some important parameters:

1) *Mean tonal preservation* : the mean value before and after filtering has been evaluating on a test homogeneous area. The new filter gives good results for the radiometric information preservation.

2) *Equivalent number of look (ENL)* : defined as E(P)^2/var(P), the ENL is a index of the speckle reduction. The higher is its value, the better is the noise removing effect. The ENL is evaluated over 5x5 homogeneous samples of the filtered images.

From these two points we can observe that:

- Lee filter and the ESTEC approach filter are the best concerning the mean tonal preservation. However the ENL in the new case is very larger than for the Lee filter.
- The new filter has the best performance in the homogeneous areas thanks to the use of the simple average (Box filter) in zones where $C_a < C_{MIN}$.
- Geometric filter is quite good in both aspects even if increases a little the mean. Instead the median filter, as predictable, even smooths well speckle, affects the mean backscatter signal value. These considerations are summarized in the Table 3.

3) *Point target preservation*: significative improvements are recognizable applying the filter around point targets. Fig. 11 show the results obtained filtering an area with two strong signals of peak/ground 8-11 dB using the different techniques. Lee filter works quite well in the homo-

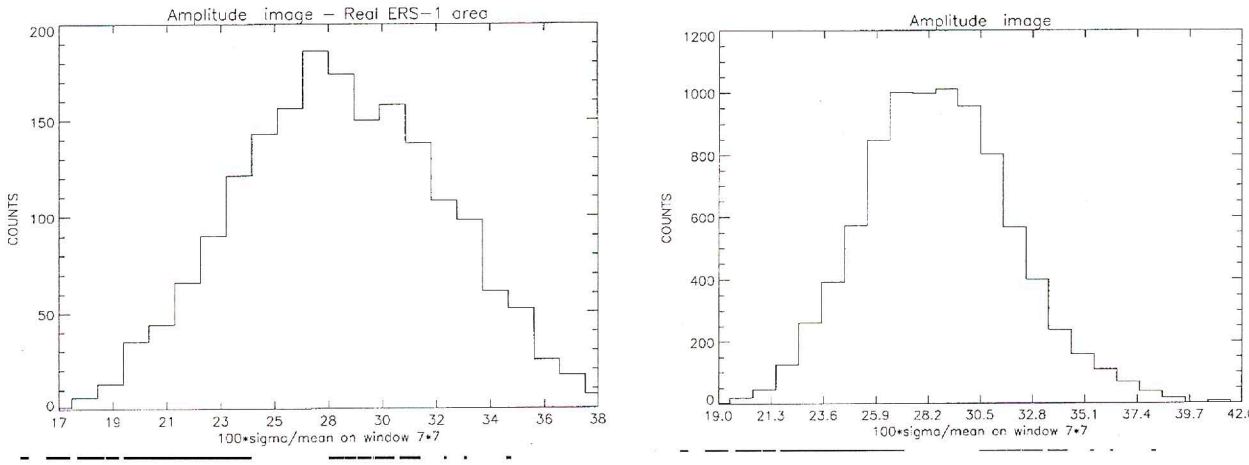

Fig. 10 - Distribution of the coefficient of variation with in a homogeneous area of a simulated 3-look image and of a real image. (a) C_{mean} *= 0.291, (b)* C_{mean}*=0.284.*

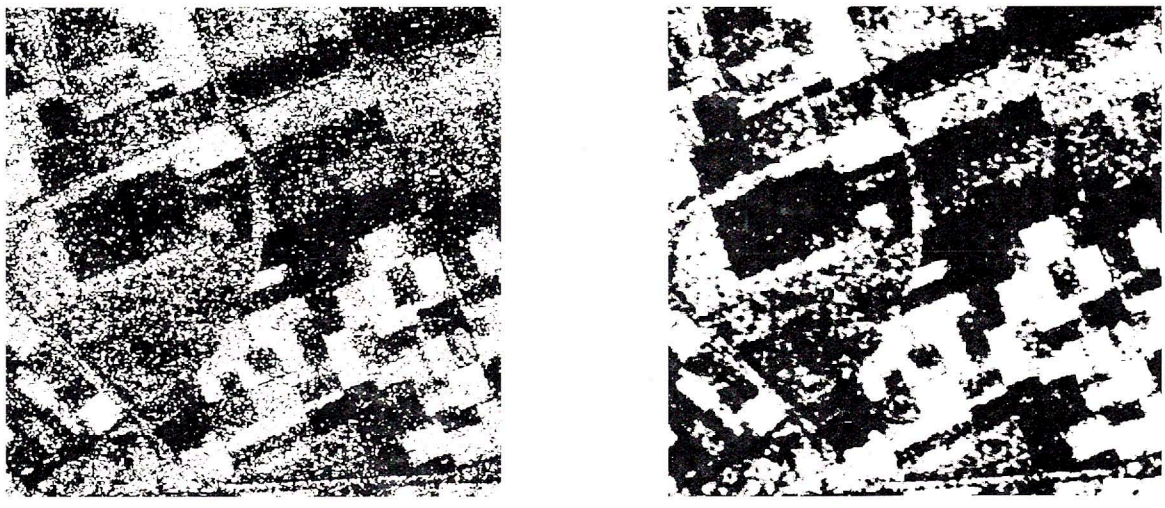

Fig. 12 - Test VMP image: (a) original image, (b) ESTEC approach filter.

geneous zone but truncate the peak's profile. Geometric filter preserves wide and spreaded high response but smears concentrated points. The median completely destroys also higher point targets. (Fig.11)

The introduction of the thresholds C_{MIN} and C_{MAX} and the spatial adaptivity allows to the ESTEC filter to adequately preserve point target responses without any efficient loss within the homogeneous areas. The plots are referring to a process with a 7x7 window. The thresholds r_{2min}=0.8 and r_{3min}=0.7 have a low Pfa_4 and correspond to a probability of detection Pd=95% for boundaries about 3 dB. C_{MAX}=0.43 is the maximum value of the C distribution computed on a simulated 3-look image using 7x7 windows. The test area, in the original version and after the filtering process, is visible in Fig. 12a and 12b.

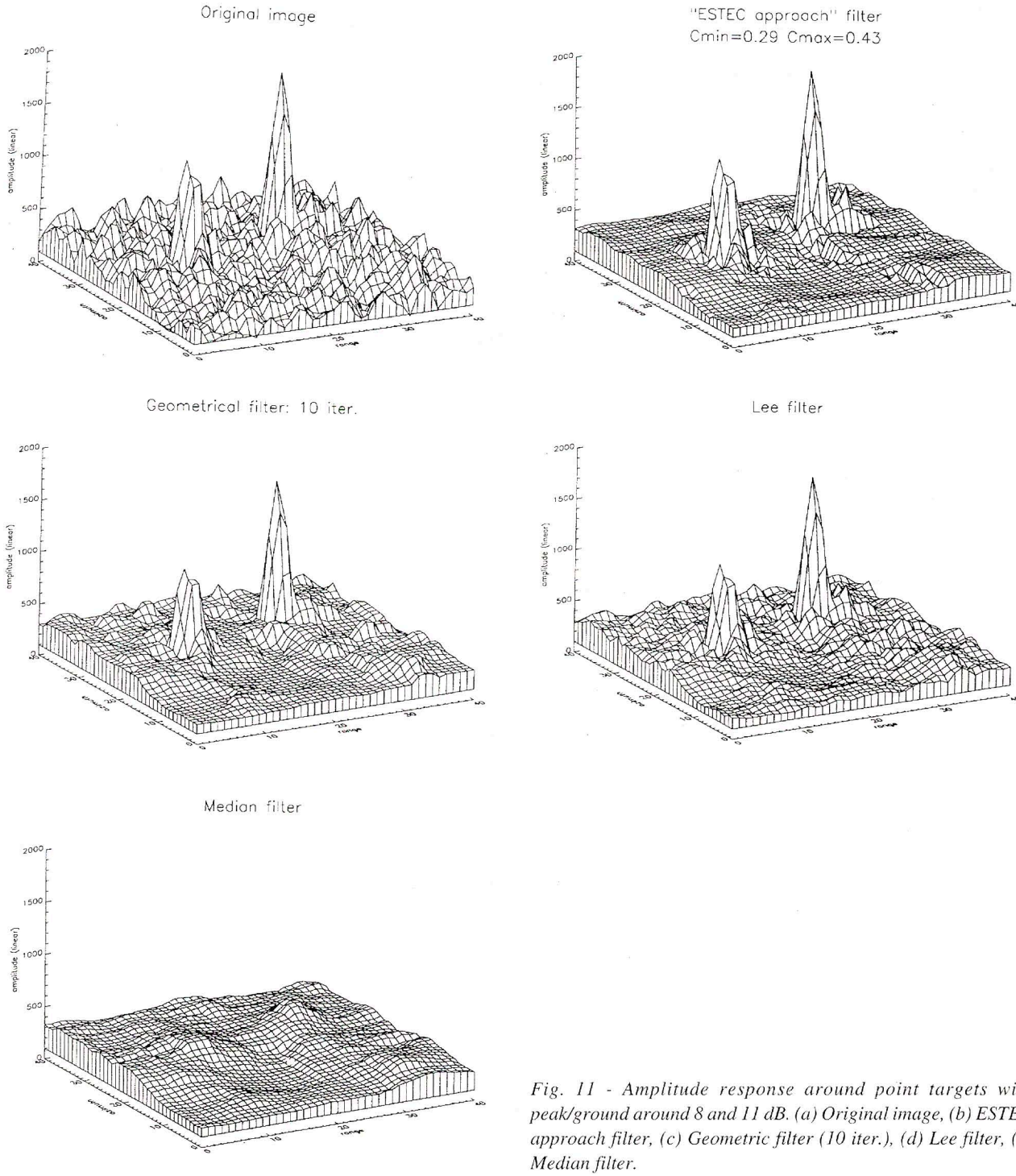

Fig. 11 - Amplitude response around point targets with peak/ground around 8 and 11 dB. (a) Original image, (b) ESTEC approach filter, (c) Geometric filter (10 iter.), (d) Lee filter, (e) Median filter.

CONCLUSIONS

Assessments of performance of different non linear filters have been proposed. A new algorithm of edge detection based on ratio operators has been tested on original and filtered ERS-1 images also taking benefit by the multitemporal data available for this satellite. Improvements of the results are evident, even if the difficulty of determining the new noise distribution after a nonlinear filtering process, doesn't allow to choose automatically the thresholds as in the case of speckled images.

Considering the disadvantages of the classical speckle filtering techniques analyzed, a different adaptive speckle filter, based on the first order statistical informations, has been applied on the images. The filter, robustly controlled by the geometrical operators and the thresholds C_{MAX} and

C_{MIN} reduces better speckle producing equivalent number of look up to 100, keeping intact the response of point targets and preserving detailes. The good filter's performance obtained from the experimental tests encourage and suggest the use of the algorithm for others applications as the display of calibrated products. Infact recent applications (Y.-L. Desnos, F.-M. Seifert, M. Loiselet, 1992) describe SAR data calibration techniques using corner reflectors and transponders situated on the ground. These devices are characterized by a high amplitude response. Then, because of the point targets preservation capability and mean tonal maintenance of the filter, is possible use also filtered images to display calibrated products.

ACKNOWLEDGEMENTS

We would like to thank J.-P. Guignard (ESA) for his support and technical comments during this work. We thank especially M. Loiselet, F.-M. Seifert and J.-L. Marchand (ESA) for their contribution at different stages of the project. We thank also A. Lopez (CESR - Toulouse France) and his team for providing us with latest publications and advised technical comments.

REFERENCES

A.C. Bovik, 1985, *Boundary Detection in Speckle Images*, Proceedings ICASSP '85, Tampa, Florida, 893-896.

T.R. Crimmins, 1985, *Geometric Filter for Speckle Reduction*, Applied Optics, Vol.24, No.10, 1438-1445.

Y.-L. Desnos, F.-M. Seifert, M. Loiselet, 1992, *A Workstation for ERS-1/JERS-1 /Multifrequency Polarimetric SAR Calibration and Validation*, IGARSS '92, Houston (TEXAS), 659-661.

P. Dewaele, P. Wambacq, A. Oesterlinck, Dic. 1989, *Speckle Reduction Techniques for SAR Images*, E.S.A.T-M.I.2, institut Montefiore/Ulg.

V.S. Frost, J.A. Stiles, K.S. Shanmugan, e J.C. Holtzman, Mar. 1982, *A Model for Radar Images and its Application to Adaptive Digital Filtering of Multiplicative Noise*, IEEE Trans. on Pattern Analysis and Machine Intell., Vol.PAMI-4, 157-166.

J.W. Goodman, Nov. 1976, *Some Fundamental of Speckle*, J. Opt. Soc. Am., Vol.66, No.11, 1145-1150.

T. Kuan, A. Sawchuk, T. Strand, P. Chavel, Mar. 1987, *Adaptive Restoration of Images with Speckle*, IEEE Trans. on Acustics speech and signal processing, Vol.ASSP-35, No.3, 373-383.

T. Kuan, A. Sawchuk, T. Strand, P. Chavel, Mar. 1985, *Adaptive Noise Smoothing Filter for Images with Signal-Dependent Noise*, IEEE Trans. Pattern Anal. Machine Intel., vol. PAMI-7, No. 2, 165-177.

J.S. Lee, May 1986, *Speckle Suppression and Analysis for Synthetic Aperture Radar Images*, Optical Engineering, Vol.25, No.5, 636-642.

J.S. Lee, 1983, *Refined Filtering of Image Noise Using Local Statistic*, Computer graphics and image processing, Vol.24, 255-269.

J.S. Lee, March 1980, *Digital Image Enhancement and Noise Filtering by Use of Local Statistic*, IEEE Trans. On Pattern Analysis and Machine Intelligence, Vol.PAMI-2, No.2, 165-168.

A. Lopes, R. Touzi, E. Nezry, Nov. 1990, *Adaptive Speckle Filters and Scene Heterogeneity*, IEEE Trans. on GRS, Vol.28, No.6, 992-1000.

A. Lopes, E. Nezry, R. Touzi, H. Laur, 1991, *Structure Detection and Statistical Adaptive Speckle Filtering in SAR Images*, (to be published).

N. Longon (Editor), 1991, *"The Data Book of ERS-1"*, ESA BR-75, Apr. 1991, ESA Pubblication Division, Noordwijk.

E. Nezry, A. Lopes, R.Touzi, Jun. 1991, *Detection of Structural and Textural Features for SAR Images Filtering*, Proc. of IGARSS'91, Espoo, Vol.4, 2169-2172.

W.K. Pratt, I.E. Abdou, May 1979, *Quantitative Design and Evaluation of Enhancement-Thresholding Edge Detectors*, Proc. IEEE, Vol.67, No.5.

R. Touzi, A. Lopes, P. Bousquet, Nov. 1988, *A Statistical and Geometrical Edge Detector for SAR Images*, IEEE Trans. on Geoscience and Remote sensing, Vol.26, No.6, 764-773.

F.T. Ulaby, A.K. Fung, R.K. Moore, *Microwave Remote Sensing, Vol.1 & 2, 1982, Vol.3, 1986, Artech House.*